Quantum Noise in Locked-type GW Interferometer and Signal Recycling

Atsushi Nishizawa (Kyoto Univ. / NAOJ-TAMA)
Collaborators :
Seiji Kawamura (NAOJ-TAMA)
Masa-aki Sakagami (Kyoto Univ.)

March 19-22, 2007,
LSC-VIRGO meeting (Adv Interf Config session)

LIGO-G070078-00-Z

Introduction

- Quantum noise
  in a recombined-type FPMI

$$S_h = \frac{{h_{SQL}}^2}{2}\left(\frac{1}{K} + K\right)$$

[Kimble et al. 2001]

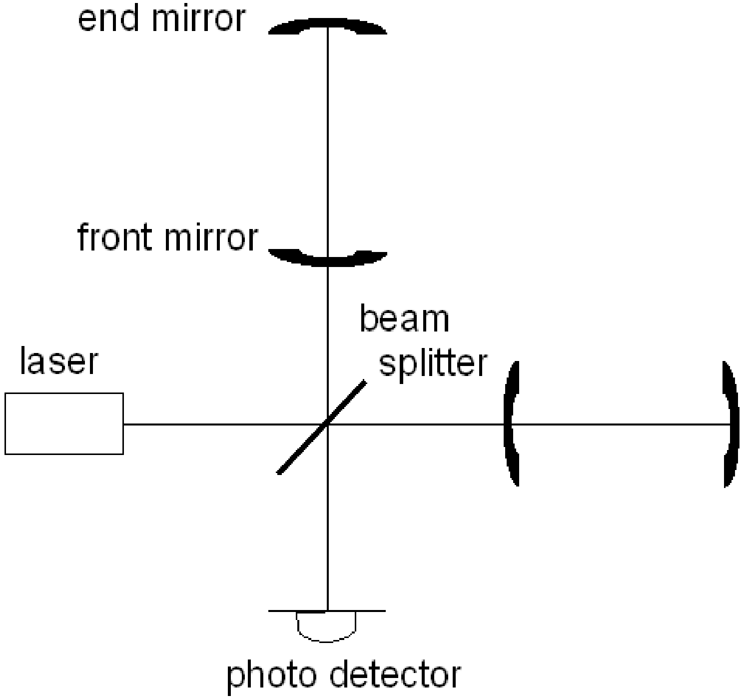

- Quantum noise
  in a recombined-type SR-FPMI

$$S_h(\Omega) = \frac{{h_{SQL}}^2}{2\tau^2 K}\frac{(C_{11}\sin\zeta + C_{21}\cos\zeta)^2 + (C_{12}\sin\zeta + C_{22}\cos\zeta)^2}{|D_1 \sin\zeta + D_2\cos\zeta|^2}$$

[Buonnano & Chen 2001]

2-dips in the noise curve

Locked-type FPM

Locked-type FPMI

- Signals are detected in each arm.
- PBS transmits the light with horizontal polarization and reflects that with vertical polarization.

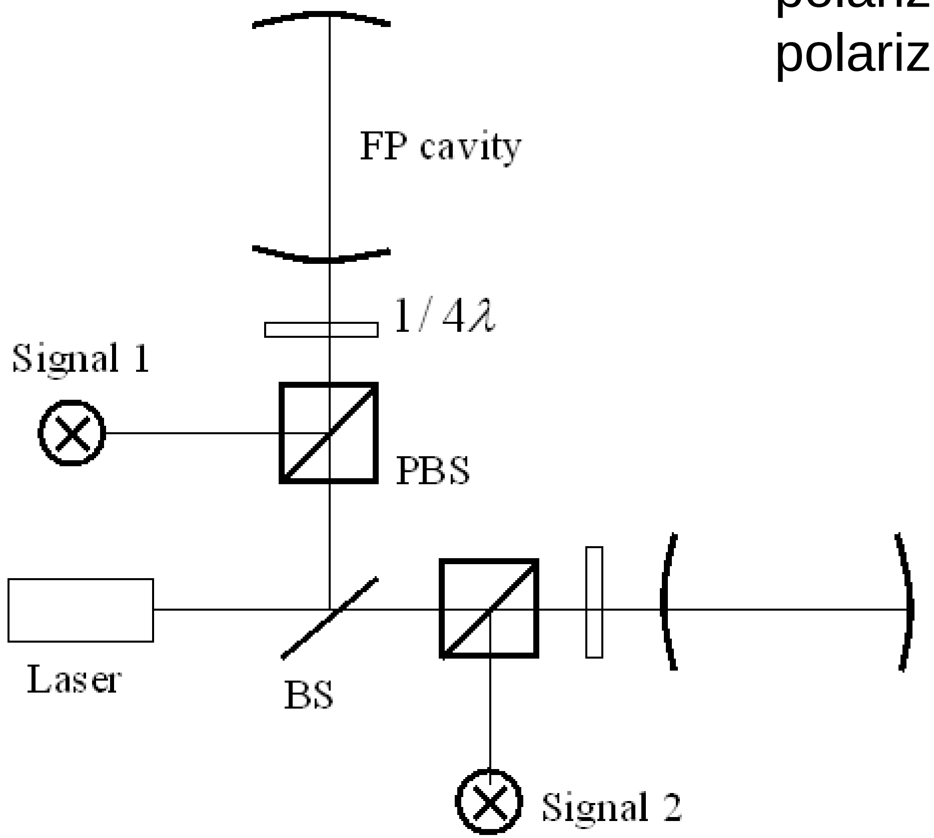

assumption

1. Cavity's end mirrors are completely reflective.
2. No phase shift for the carrier light other than in the FP cavity.
3. Negligible phase shift for the sideband except in FP cavity.
4. All optics are lossless.

Vacuum fluctuations injected into the IFO

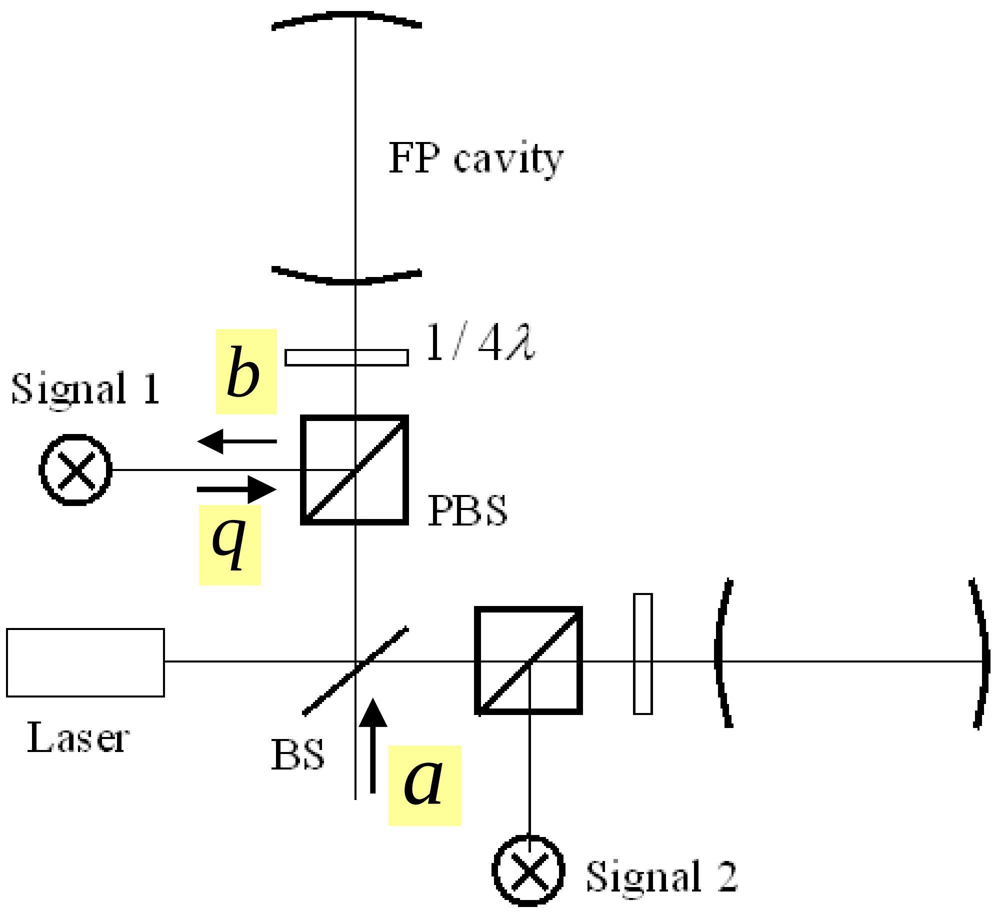

Vacuum fluctuations injected into the IFO

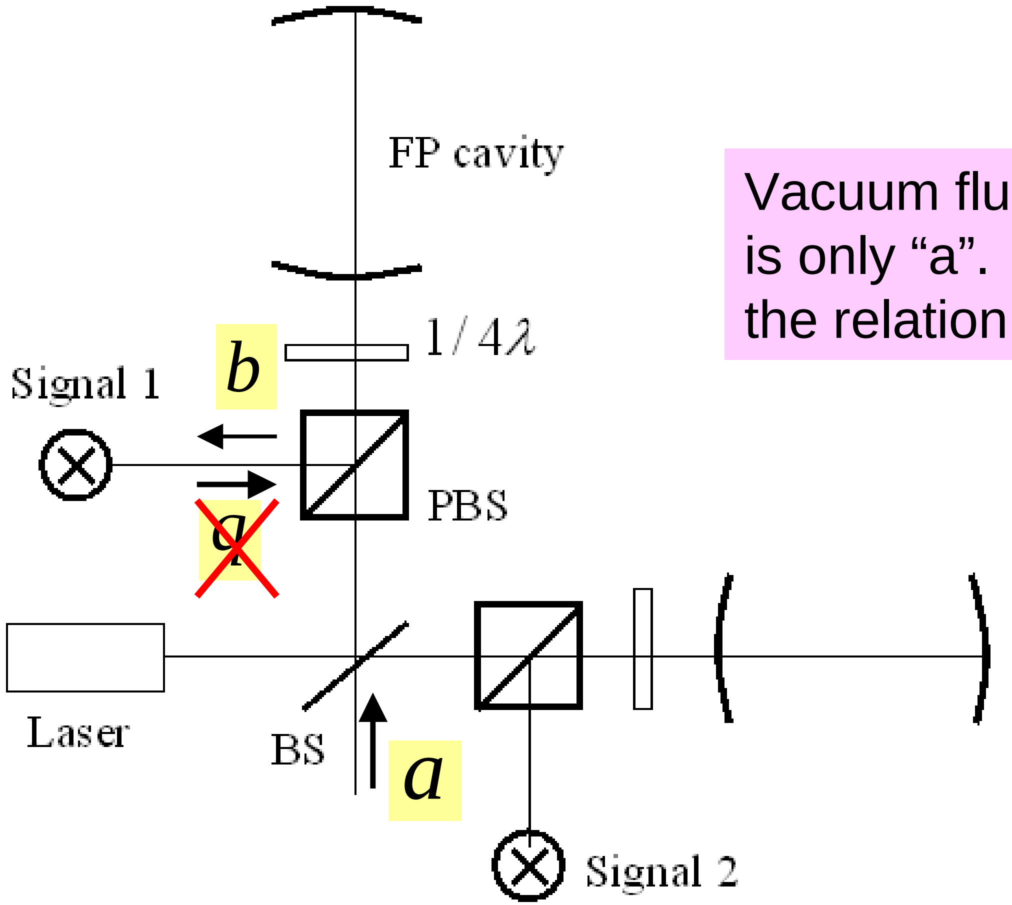

Vacuum fluctuation injected into this IFO is only “a”. What we want to know is the relation between “a” and “b”

Vacuum fluctuations injected into the IFO

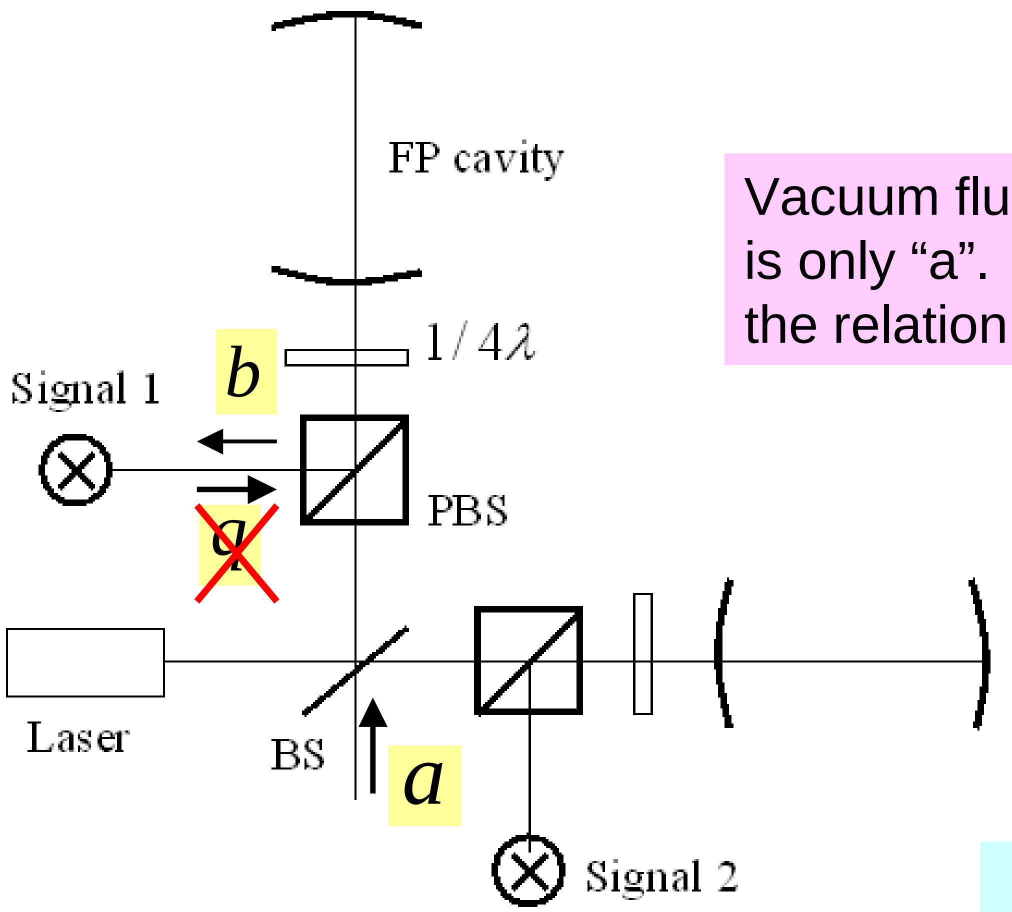

Vacuum fluctuation injected into this IFO is only “a”. What we want to know is the relation between “a” and “b”

$$S_h(\Omega) = \frac{h_{SQL}{}^2}{2}\left(\frac{1}{K} + K\right)$$

Locked-type SR-FPMI

Putting SR mirrors

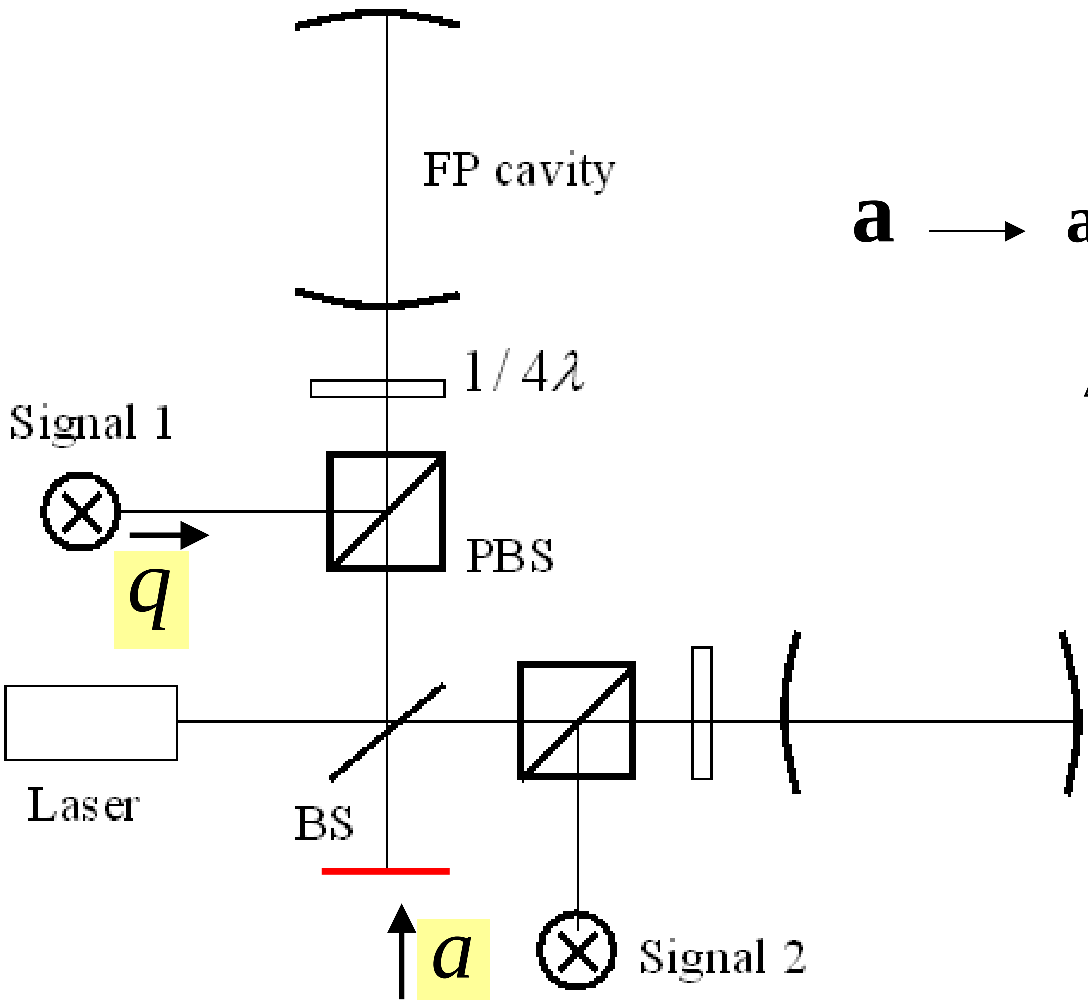

$$\mathbf{a} \longrightarrow \mathbf{a}' = \frac{1}{\sqrt{2}} e^{2i\beta} \Delta\mathbf{q}$$

$$\Delta\mathbf{q} \equiv \mathbf{q}^n - \mathbf{q}^e$$

Putting SR mirrors

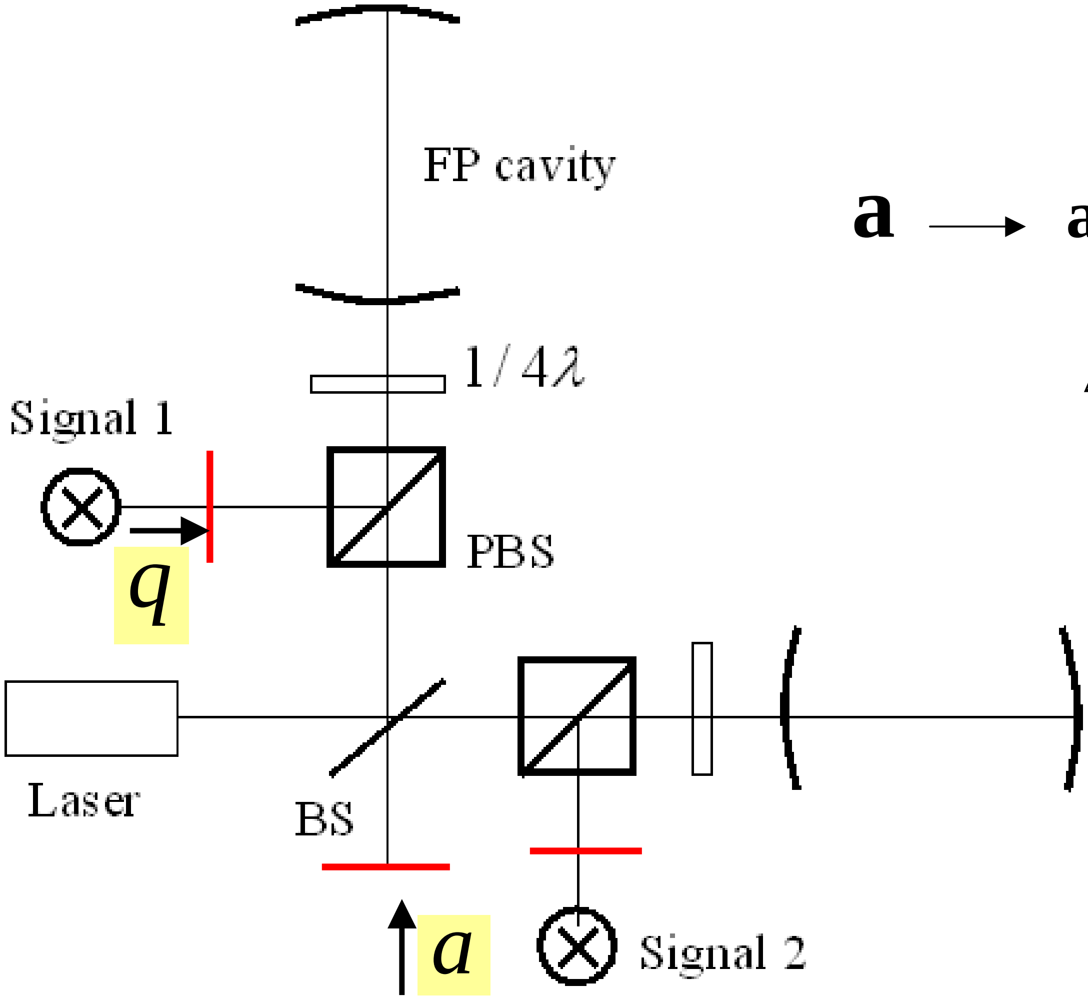

$$\mathbf{a} \longrightarrow \mathbf{a}' = \frac{1}{\sqrt{2}} e^{2i\beta} \Delta\mathbf{q}$$

$$\Delta\mathbf{q} \equiv \mathbf{q}^n - \mathbf{q}^e$$

SR cavity

$$\phi \equiv [\omega_0 \ell / c]_{\mathrm{mod}(2\pi)}$$

darkport cavity

$$\theta \equiv [\omega_0 \ell_d / c]_{\mathrm{mod}(2\pi)}$$

Sensitivity curve

$$S_h(\Omega) = \frac{h_{SQL}{}^2}{2\tau^2 K} \frac{(C_{11}\sin\zeta + C_{21}\cos\zeta)^2 + (C_{12}\sin\zeta + C_{22}\cos\zeta)^2}{|D_1 \sin\zeta + D_2\cos\zeta|^2}$$

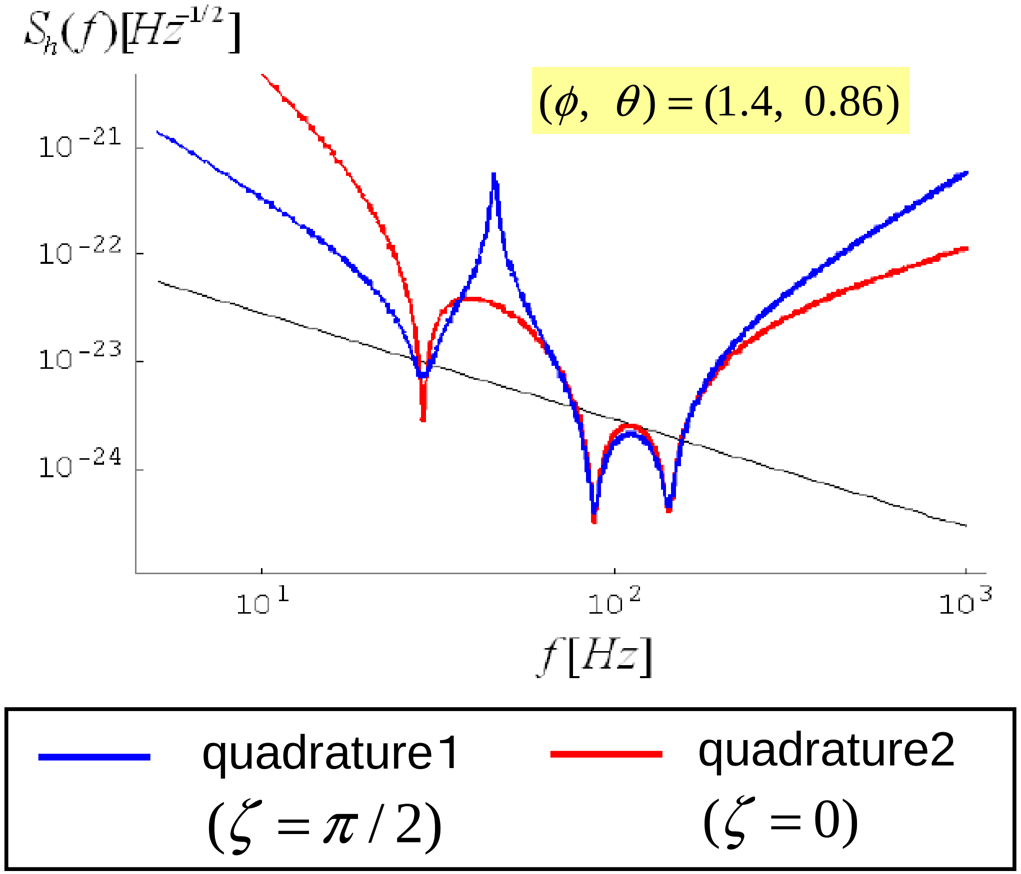

Arm length $3\,km$

Mirror mass $30\,kg$

Laser wavelenth $1.064\,\mu m$

Laser power

$$I_0 = I_{SQL} = 2162\,W$$

FP cavity's Mirror transmissivity

$$T = 0.14$$

SR mirror reflectivity

$$\rho = 0.98$$

LIGO-G070078-00-Z

Interpretation of dips

Decomposition of spectral density

$q^n - q^e$

$$\Delta \mathbf{b} = \frac{1}{M}\left[e^{4i\beta}\begin{pmatrix} C_{11} & C_{12} \\ C_{21} & C_{22}\end{pmatrix}\Delta \mathbf{q} + 2\tau\sqrt{K}e^{i\beta}\begin{pmatrix} D_1 \\ D_2\end{pmatrix}\frac{h}{h_{SQL}}\right]$$

$b^n - b^e$

Noise signal   GW signal

normalization

$$\mathcal{O}_i(\Omega) = \mathcal{Z}_i(\Omega) + R_{xx}\mathcal{F}_i(\Omega) + Lh(\Omega)$$

$i = 1,2$

shot $\propto 1/\sqrt{I_0}$

radiation $\propto \sqrt{I_0}$

GW

$$R_{xx}(\Omega) = -\frac{4}{m\Omega^2}$$

$$S_h = \frac{1}{L^2}\left[S_{\mathcal{Z}\mathcal{Z}} + R_{xx}^2 S_{\mathcal{F}\mathcal{F}} + 2R_{xx}S_{\mathcal{Z}\mathcal{F}}\right]$$

Analyzing each term will gives the interpretation of the dips.

The number of dips

$S_h = 0$ → $\sqrt{\bar{S}_{\mathcal{Z}_i \mathcal{Z}_i}} = -R_{xx} \sqrt{\bar{S}_{\mathcal{F}_i \mathcal{F}_i}}$

$$y \equiv \left(\frac{\Omega_{res}}{\gamma}\right)^2$$

$$y\left[(1+y)^2\, cos2(\theta+\phi) - (1-6y+y^2)\right]$$
$$= 2n\left[(1+y)\, sin2(\theta+\phi) + (1-y)\, (sin2\theta + sin2\phi)\right]$$

$$n \equiv I_0/I_{SQL}$$

The number of dips

$S_h = 0$ $\Rightarrow$ $\sqrt{\bar{S}_{\mathcal{Z}_i\mathcal{Z}_i}} = -R_{xx}\sqrt{\bar{S}_{\mathcal{F}_i\mathcal{F}_i}}$

$$y \equiv \left(\frac{\Omega_{res}}{\gamma}\right)^2$$

$$y\left[(1+y)^2\, cos2(\theta+\phi) - (1-6y+y^2)\right]$$
$$= 2n\left[(1+y)\, sin2(\theta+\phi) + (1-y)\,(sin2\theta + sin2\phi)\right]$$

$$n \equiv I_0/I_{SQL}$$

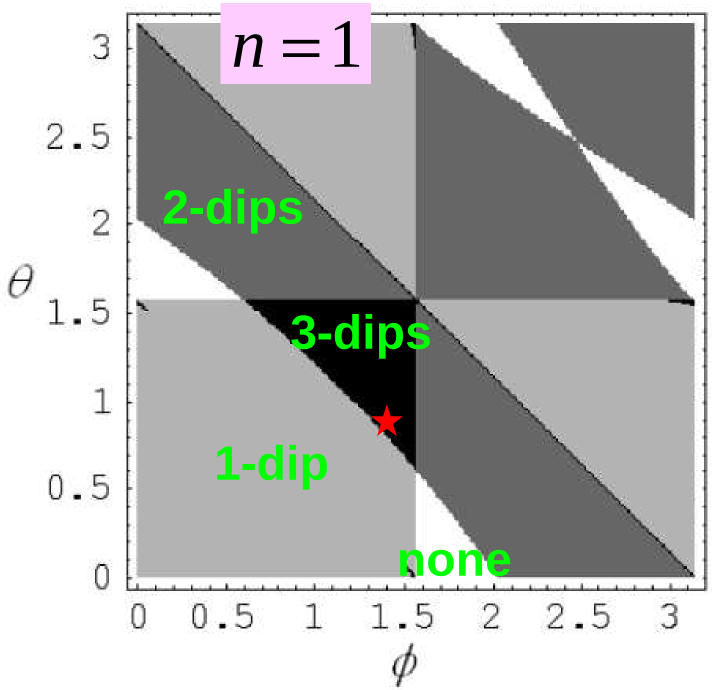

The number of dips depends on θ and ϕ .

The number of dips

$S_h = 0$ ⇒ $\sqrt{\bar{S}_{\mathcal{Z}_i\mathcal{Z}_i}} = -R_{xx}\sqrt{\bar{S}_{\mathcal{F}_i\mathcal{F}_i}}$

$$y\left[(1+y)^2\, cos2(\theta+\phi) - (1-6y+y^2)\right] = 2n\left[(1+y)\, sin2(\theta+\phi) + (1-y)\,(sin2\theta + sin2\phi)\right]$$

$$y \equiv \left(\frac{\Omega_{res}}{\gamma}\right)^2$$

$$n \equiv I_0/I_{SQL}$$

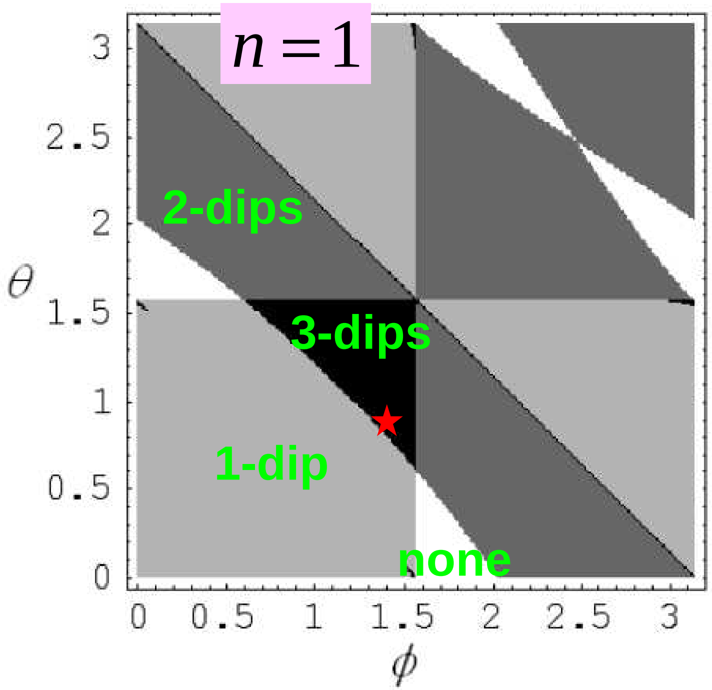

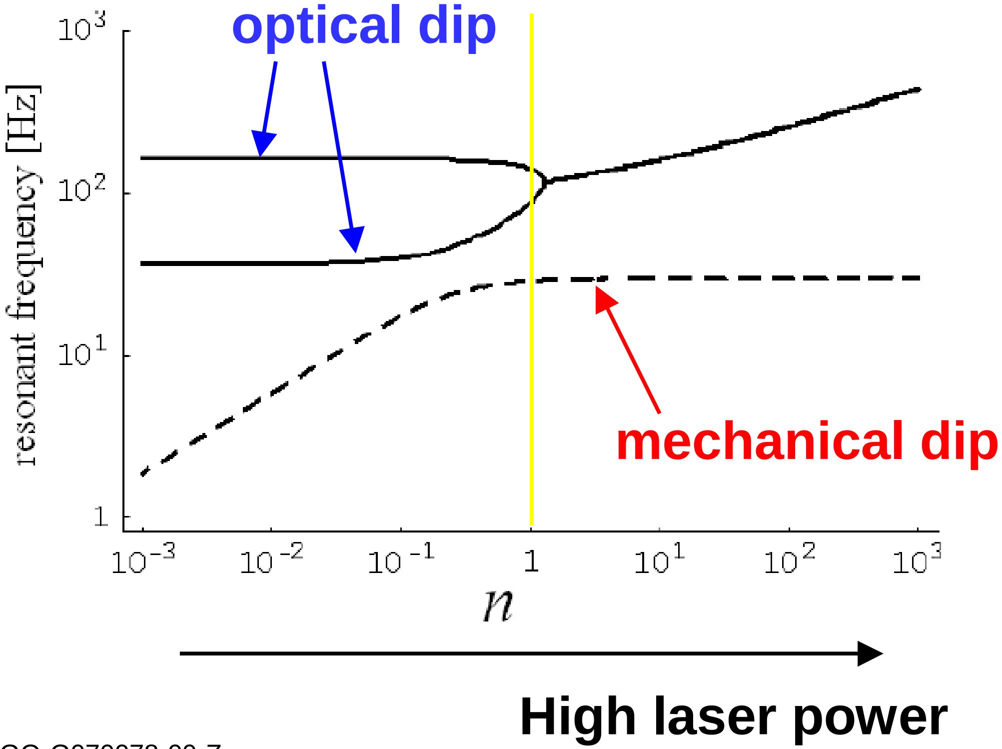

The number of dips depends on θ and ϕ !

The reason for the increase of optical dips

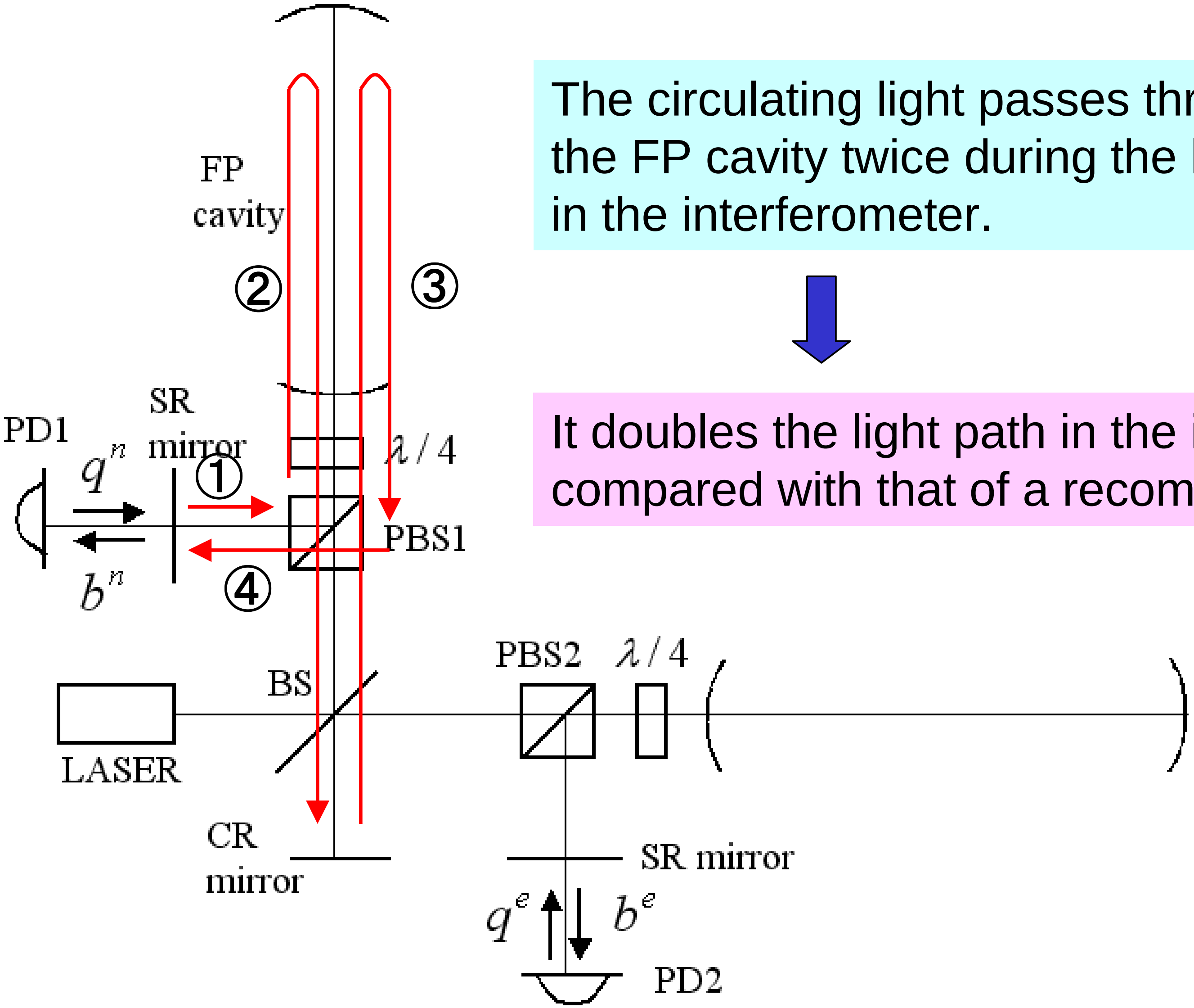

The circulating light passes through the FP cavity twice during the light trip in the interferometer.

It doubles the light path in the interferometer compared with that of a recombined-type.

The reason for the increase of optical dips

$S_{Z1Z1} = 0, \;\; S_{Z2Z2} = 0$

recombined type

$$\cos 2\beta = \cos 2\phi$$

$$\rightarrow \pm 2\beta + 2\pi\ m = 2\phi$$

$$\rightarrow \pm \arctan(\Omega / \gamma) - \phi = \pi\ m$$

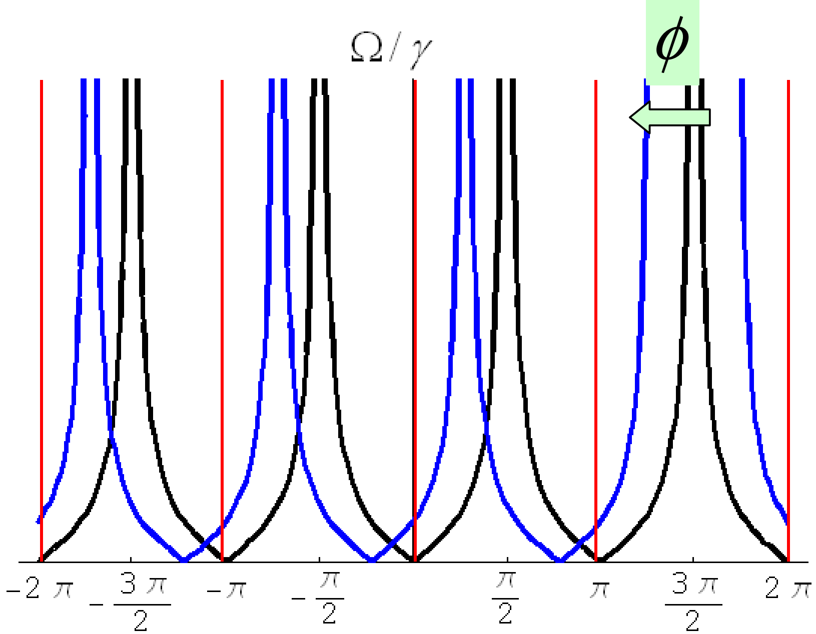

locked type

$$\cos 4\beta = \cos 2(\phi + \theta)$$

$$\rightarrow \pm 4\beta + 2\pi\ m = 2(\phi + \theta)$$

$$\rightarrow \pm 2\arctan(\Omega / \gamma) - (\phi + \theta) = \pi\ m$$

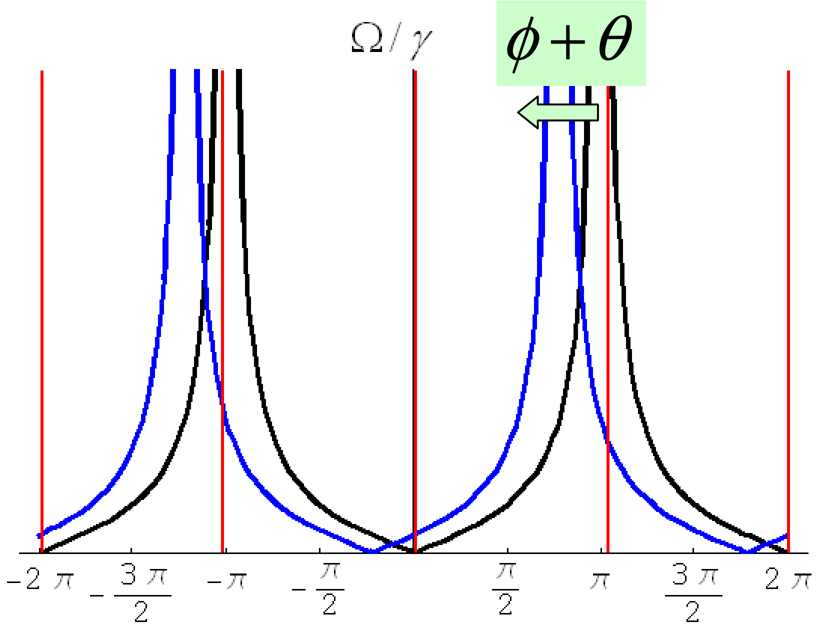

Comparison with recombined-type

Comparison of Inspiral range with Adv-LIGO

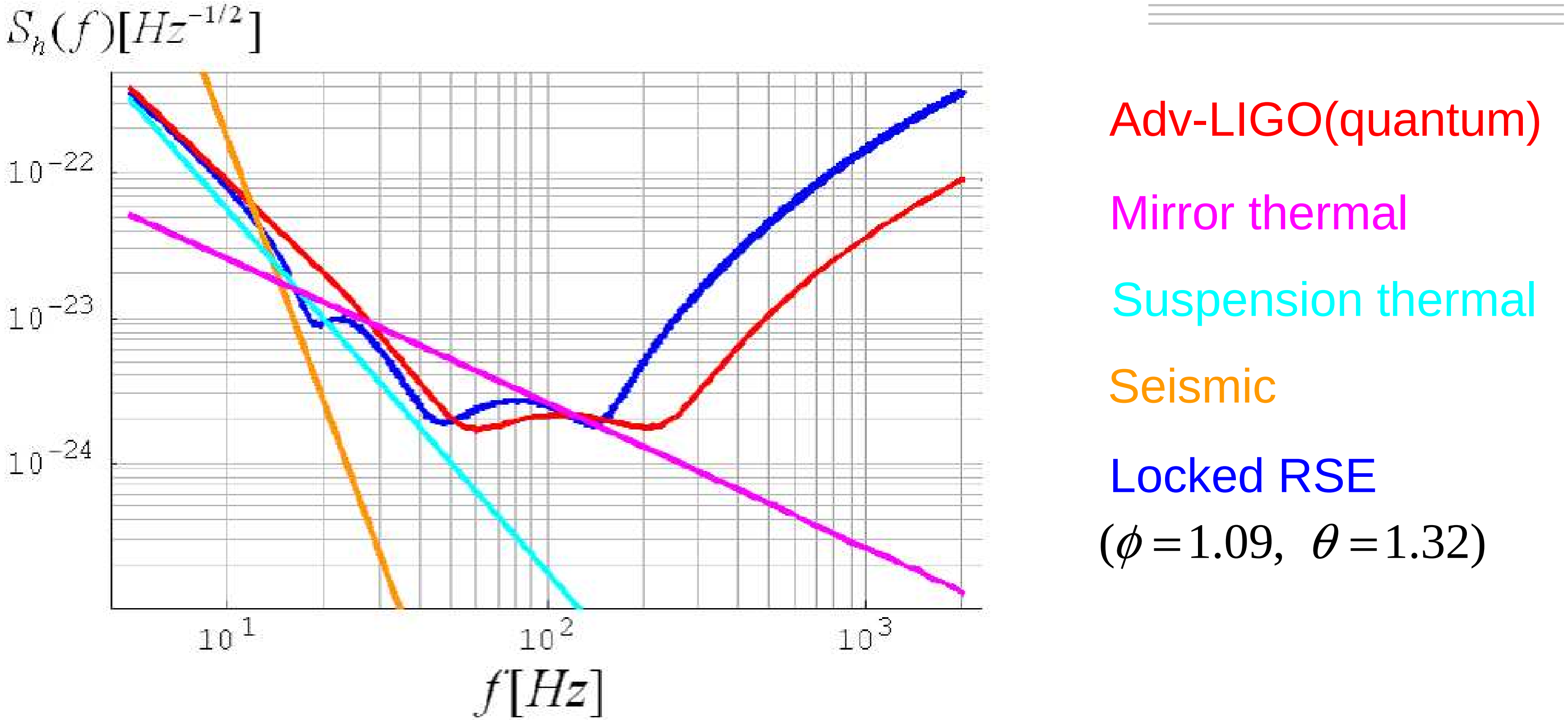

configuration	NS binary	BH binary ($50M_\odot$)	BH binary ($100M_\odot$)
Advanced-LIGO	1	1	1
Locked-type (blue)	0.90	1.05	1.24

Classical noise impairs the advantage of the locked-type RSE.
But, lower classical noise allows us to improve the sensitivity.

Comparison of Inspiral range with LCGT

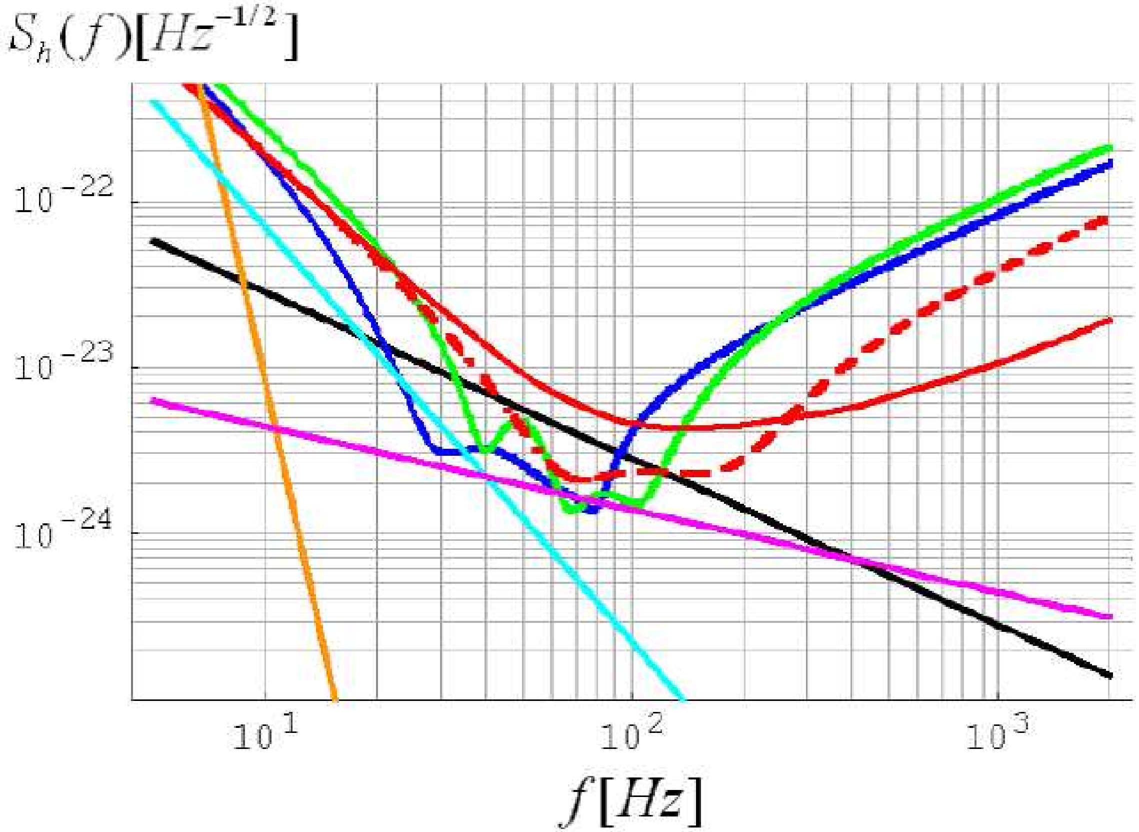

LCGT(tuned, detuned)

Mirror thermal

Suspension thermal

Seismic

SQL

Locked RSE1

$(\phi = 0.13,\ \theta = 1.49)$

Locked RSE2

$(\phi = 1.38,\ \theta = 0.61)$

configuration	NS binary	BH binary ($50M_\odot$)	BH binary ($100M_\odot$)
LCGT (broadband)	1	1	1
LCGT (narrowband)	1.25	1.56	1.17
Locked-type (brue)	1.43	2.28	2.94
Locked-type (green)	1.30	1.87	1.81

Summary

- We considered **quantum noise in a locked-type FPMI** and applied **signal recycling** to it.

- There appears at most **3 dips** in the sensitivity curve.

- Then, applying locked-type RSE to a real IFO and making the third dip in low frequency, gives **the improvement of the SNR for binaries** by the factor **1.4 - 2.9**.

- It is important to reduce the classical noise level (particularly, thermal noise) in order to take advantage of the quantum technique.

The END

終

Input –output relation

$$\Delta \mathrm{b} = \frac{1}{M}\left[e^{4i\beta}\begin{pmatrix} C_{11} & C_{12} \\ C_{21} & C_{22}\end{pmatrix}\Delta \mathrm{q} + 2\tau\sqrt{K}e^{i\beta}\begin{pmatrix} D_1 \\ D_2 \end{pmatrix}\left(\frac{h}{h_{SQL}}\right)\right]$$

$$\begin{aligned} M &= 1+\rho^2 e^{8i\beta} \\ &\quad -2\rho\, e^{4i\beta}\left[cos2(\theta+\phi)+\frac{K}{2}\left\{(1+\rho^2)\ sin2(\theta+\phi)+(e^{-2i\beta}+\rho^2 e^{2i\beta})\ sin2\theta+2\rho\ cos2\beta\ sin2\phi\right\}\right] \end{aligned}$$

$$\begin{aligned} C_{11} &= (1+\rho^2)\ cos2(\theta+\phi)-2\rho\ cos4\beta \\ &\quad +\frac{K}{2}\left[(1+\rho^2)^2\ sin2(\theta+\phi)-\tau^4\ sin2\theta+2\rho\ cos2\beta\{(1+\rho^2)\ sin2\phi+2\rho\ sin2\theta\}\right] \end{aligned}$$

$$\begin{aligned} C_{22} &= (1+\rho^2)\ cos2(\theta+\phi)-2\rho\ cos4\beta \\ &\quad +\frac{K}{2}\left[(1+\rho^2)^2\ sin2(\theta+\phi)+\tau^4\ sin2\theta+2\rho\ cos2\beta\{(1+\rho^2)\ sin2\phi+2\rho\ sin2\theta\}\right] \end{aligned}$$

$$C_{12} = -\tau^2\left[sin2(\theta+\phi)+K\ sin\phi\ \{(1+\rho^2)\ sin(2\theta+\phi)+2\rho\ cos2\beta\ sin\phi\}\right]$$

$$C_{21} = \tau^2\left[sin2(\theta+\phi)-K\ cos\phi\ \{(1+\rho^2)\ cos(2\theta+\phi)+2\rho\ cos2\beta\ cos\phi\}\right]$$

$$D_1 = -\left[(1+\rho^2 e^{6i\beta})\ sin\phi+2\rho\ e^{3i\beta}\ cos\beta\ sin(2\theta+\phi)\right]$$

$$D_2 = -\left[(-1+\rho^2 e^{6i\beta})\ cos\phi+2i\rho\ e^{3i\beta}\ sin\beta\ cos(2\theta+\phi)\right]\ .$$

Decomposition of spectral density

Assuming $\tau << 1$ and taking the leading term about τ ,

$$\bar{S}_{\mathcal{Z}_1\mathcal{Z}_1} = \frac{2L^2h_{SQL}^2}{\tau^2 K|D_1|^2}[cos2(\theta+\phi) - cos4\beta]^2$$

$$\bar{S}_{\mathcal{F}_1\mathcal{F}_1} = \frac{2L^2h_{SQL}^2 K}{\tau^2 R_{xx}^2|D_1|^2} \times [sin2(\theta+\phi) + cos2\beta\{sin2\theta + sin2\phi\}]^2$$

$$\bar{S}_{\mathcal{Z}_1\mathcal{F}_1} = S_{\mathcal{F}_1\mathcal{Z}_1} = -\frac{2L^2h_{SQL}^2}{\tau^2 R_{xx}|D_1|^2}[cos2(\theta+\phi) - cos4\beta] \times [sin2(\theta+\phi) + cos2\beta\{sin2\theta + sin2\phi\}]$$

$D_1 \rightarrow D_2$ gives the spectral density for the other quadrature.

Numerator =0 ⟶ The dip of quantum noise

Denominator =0 ⟶ GW suppression

Decomposition of spectral density

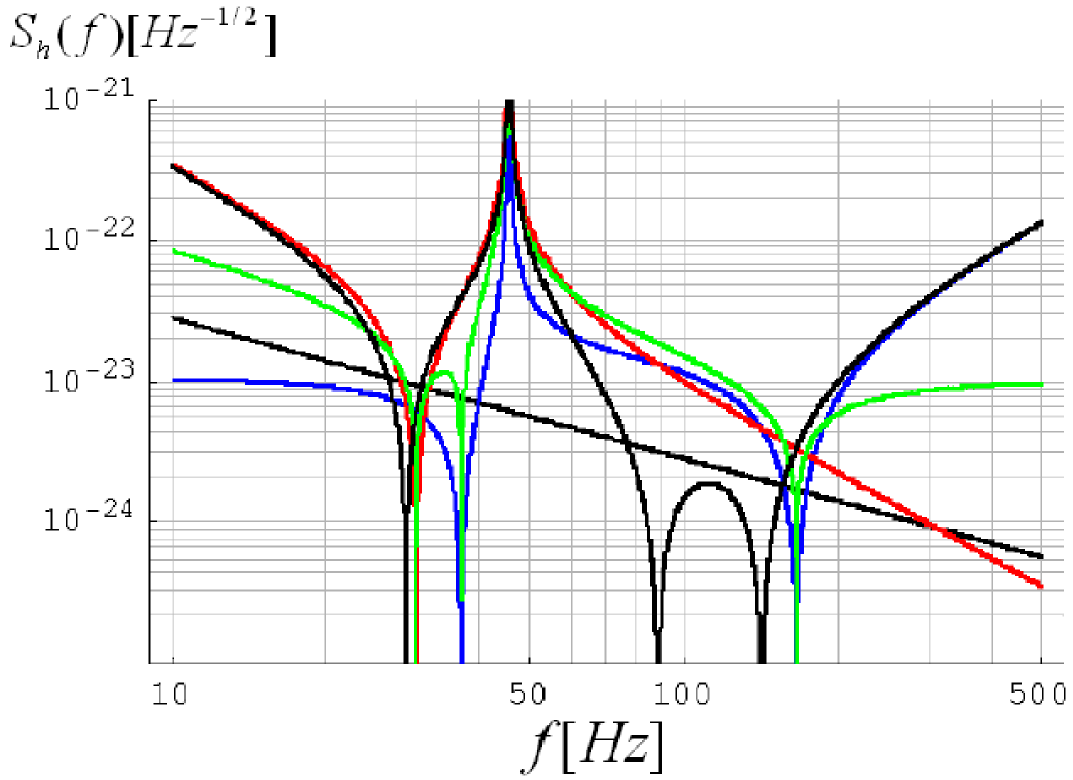

Arm length $3km$

Mirror mass $30kg$

Laser wavelenth $1.064\,\mu m$

Laser power

$$I_0 = I_{SQL} = 2162W$$

FP cavity's Mirror transmissivity

$$T = 0.14$$

SR mirror reflectivity

$$\rho = 0.98$$

Blue: S_{Z1Z1}/L^2	Green: $2\lvert R_{xx} S_{Z1F1}\rvert / L^2$
Red: $R_{xx}{}^2 S_{F1F1}/L^2$	Black: $S_h(total)$

The number of dips

$S_{Z1Z1} = 0,\ S_{Z2Z2} = 0$

$$1 - 6y + y^2 = (1+y)^2\, cos2(\theta + \phi)\ . \qquad y \equiv \left(\frac{\Omega_{res}}{\gamma}\right)^2$$

$$\Rightarrow \quad y_s = \frac{3 + cos2(\theta+\phi) \pm 2\sqrt{2\{1 + cos2(\theta+\phi)\}}}{1 - cos2(\theta+\phi)}\ .$$

2 real solutions（when $2(\theta+\phi) = \pi$, degenerated sonlution）

$$S_h = \frac{1}{L^2}[S_{\mathcal{Z}\mathcal{Z}} + R_{xx}^2 S_{\mathcal{F}\mathcal{F}} + 2R_{xx}S_{\mathcal{Z}\mathcal{F}}] \xrightarrow[I_0 / I_{SQL} \to 0]{} S_h = S_{ZZ} / L^2$$

$\Rightarrow$ 2 optical dips

GW suppression

$D_1 = 0$ $$(1+y)[sin(2\theta+\phi) - sin\phi] + 2(1-y)sin\phi = 0$$

$$\Rightarrow \quad y_{GW}^{(1)} = \frac{sin\phi + sin(2\theta+\phi)}{3sin\phi - sin(2\theta+\phi)}$$

$D_2 = 0$ $$(1+y)[cos(2\theta+\phi) + cos\phi] + 2(1-y)cos\phi = 0$$

$$\Rightarrow \quad y_{GW}^{(2)} = \frac{3cos\phi + cos(2\theta+\phi)}{cos\phi - cos(2\theta+\phi)}$$

$D_1 = 0$

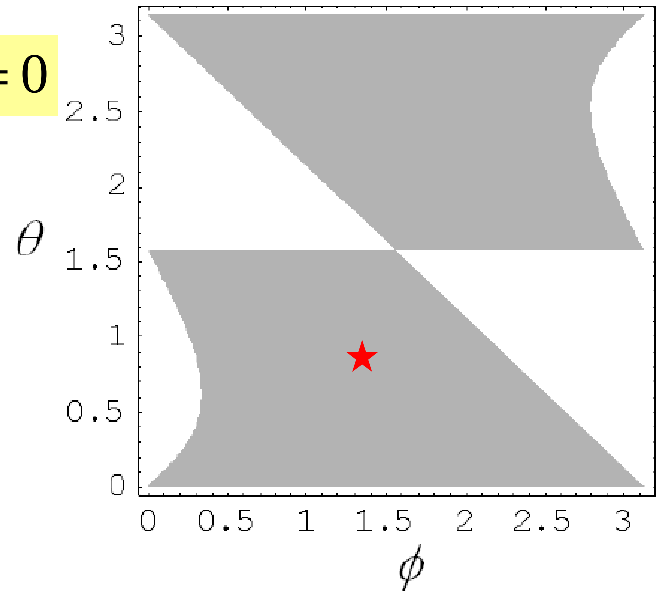

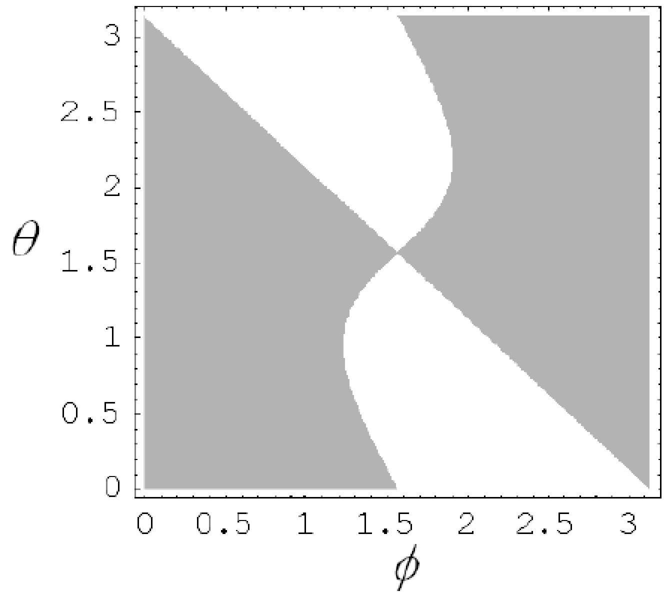

$D_2 = 0$

Validity of the high reflectivity approximation

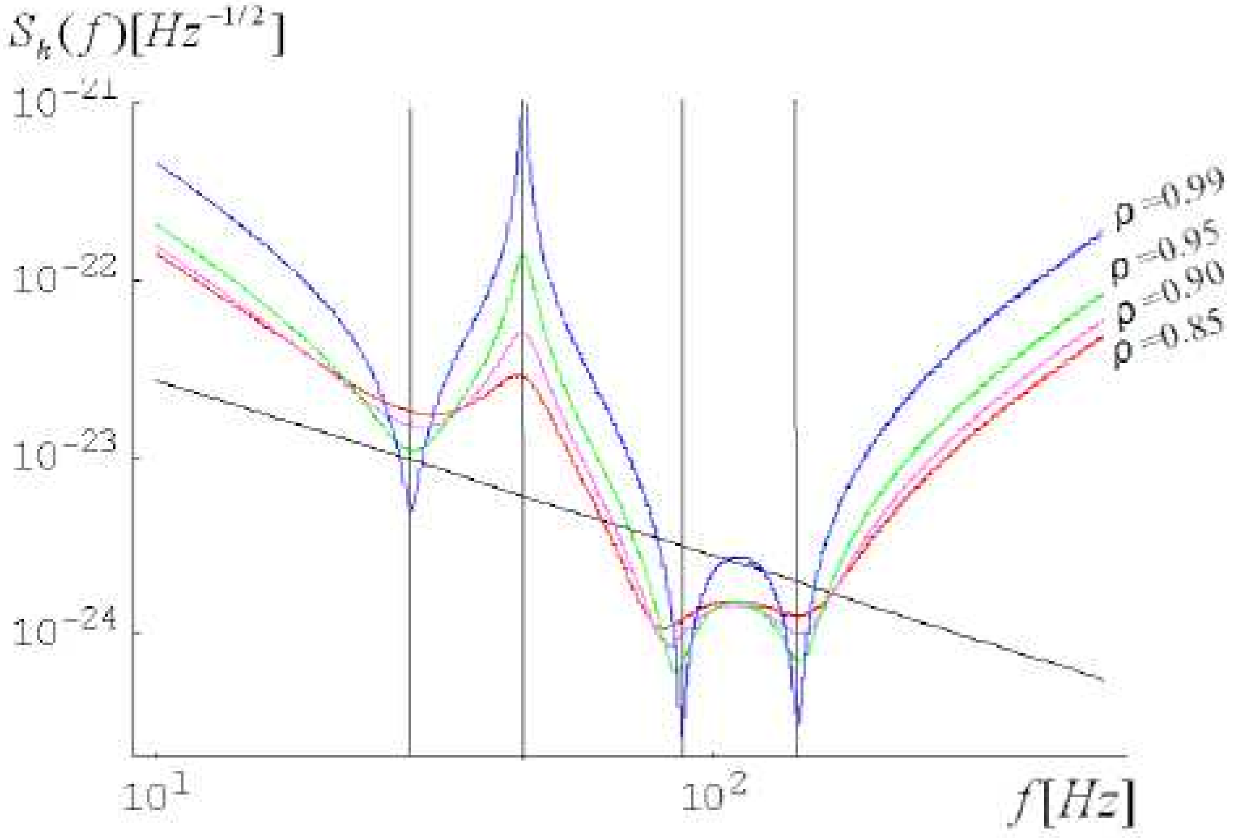

- Larger ρ makes the deeper dips.
- The resonant frequencies of a full calculation greatly agree with that in the approximation.

Inspiral range of binaries

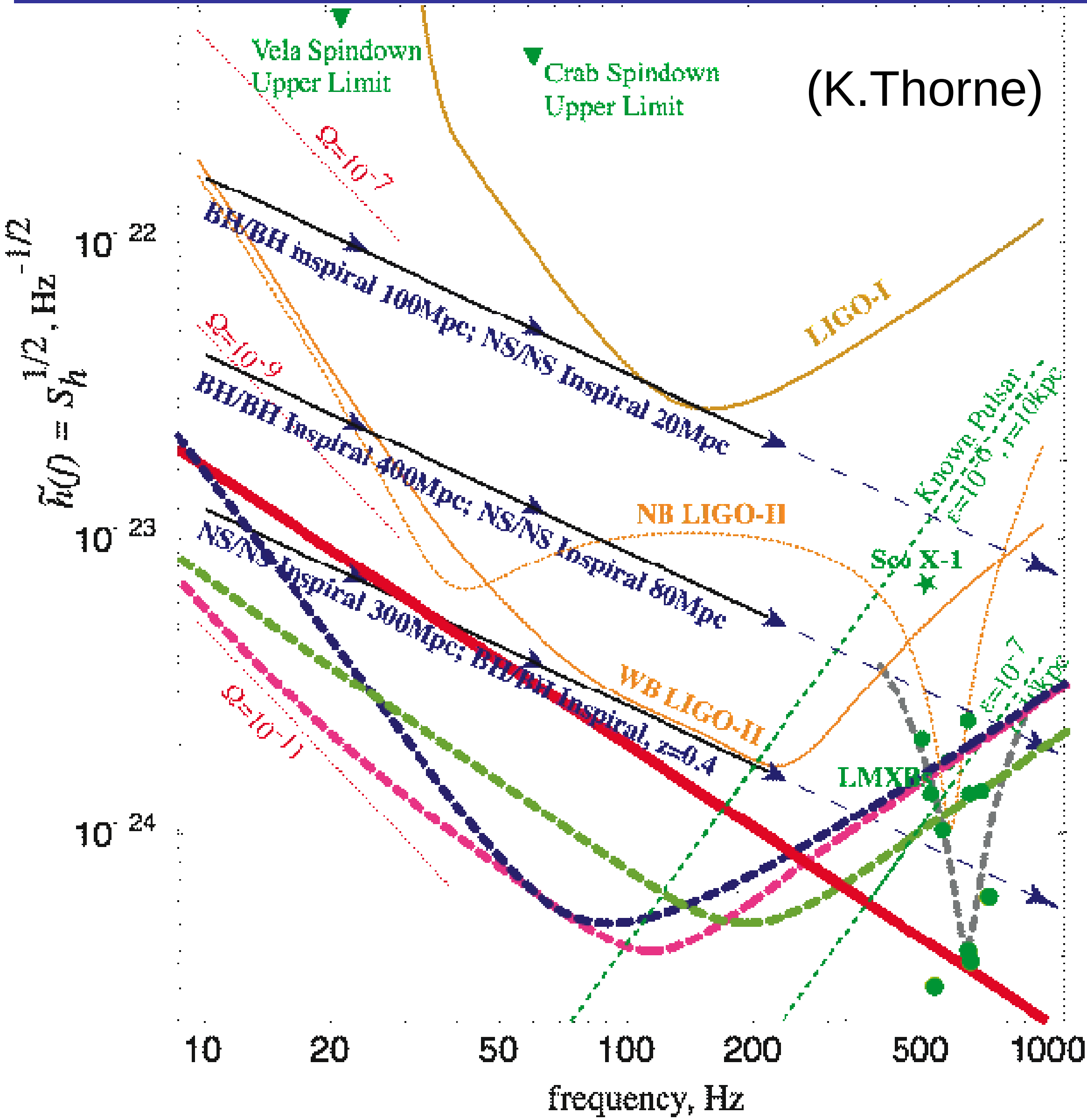

Fourier component

$$|\tilde{h}(f)|^2 \propto f^{-7/3}$$

$$(SNR)^2 = 4\int_0^\infty \frac{|\tilde{h}(f)|^2}{S_h(f)} df$$

(Flanagan & Hughes 1998)

Parameters for Inspiral Range Calculation

parameter

configuration	T	ρ	ϕ	θ	ζ
Advanced-LIGO	0.0707	0.96	1.51	—	$\pi/2$
Locked-type (green)	0.1400	0.78	1.09	1.32	$\pi/2$
LCGT (broadband)	0.0632	0.88	$\pi/2$	—	$\pi/2$
LCGT (narrowband)	0.0632	0.95	1.49	—	0.80
Locked-type (green)	0.1400	0.59	0.13	1.49	1.00
Locked-type (brue)	0.1400	0.85	1.38	0.61	2.74

SNR

configuration	NS binary	BH binary ($50M_\odot$)	BH binary ($100M_\odot$)
Advanced-LIGO	1	1	1
Locked-type (blue)	0.90	1.05	1.24
LCGT (broadband)	1	1	1
LCGT (narrowband)	1.25	1.56	1.17
Locked-type (brue)	1.43	2.28	2.94
Locked-type (green)	1.30	1.87	1.81